Supporting Information

Pan et al. 10.1073/pnas.1011711108

SI Results

Elimination of *C. elegans* nuclear membrane components shortens lifespan (1). Because animals lacking both the maternal and zygotic components of the nuclear membrane protein LMN-1/lamin are not viable, we analyzed mutants lacking the zygotic but retaining the maternal LMN-1, *lmn-1* (M+Z-). Similar to *daf-16* and *hsf-1* mutants, *lmn-1* (M+Z-) animals had shortened lifespan (1) and accelerated touch neuron aging (D1, no touch receptor neuron defects, $n = 15$; D4, ALM defects, 16%, $n = 19$; PLM defects, 11%, $n = 19$; D6, ALM defects, 52%, $n = 21$; $P = 0.0000068$, PLM defects, 57%, $n = 23$, $P = 0.00009$, Fisher's exact test).

SI Materials and Methods

The following *Caenorhabditis elegans* alleles and transgenes were used in the current study: LGI: *daf-16(mu86)* (2), *hsf-1(sy441)* (3), *mec-6(e1342)* (4), *lmn-1(tm1502)/hT2)* (1), *unc-13(e1091)*, *zdIs5[Pmec-4::gfp, lin-15(+)]* (5); LGII: *eat-2(ad465)* (6), *muIs32[Pmec-7::gfp, lin-15(+)]*, *juIs76[Punc-25::gfp, lin-15(+)]*; LGIII: *daf-2(e1368)*, *daf-2(e1370)* (7), *mec-12(e1605)* (8); LGIV: *fbl-1(hd43)/dpy-20(e1282) unc-24(e138)* (9), *zIs356[Pdaf-16::daf-16::gfp, rol-6(su1006)]* (10); LGV: *mec-1(e1066)*, *mec-1 (e1292)*, *mec-1(e1526)*, *mec-9(e1494)* (all from ref. 8), *slo-1 (js118)* (11), *slo-1(ky389)*, *slo-1(ky399)* (all from ref. 12), *Punc-17::rfp* (13); LGX: *mec-2(e75)* (8), *mec-4(u253)* (14), *mec-5 (e1340)* (8), *mec-10(e1515)* (8), *him-4(rh319)* (9), *unc-18(e234)*, *dgk-1(sy428)*; linkage group undetermined: *muIs126[Pmyo-3::gfp::daf-16*, *rol-6(su1006)]*, *muIs131[Punc-119::gfp::daf-16, rol-6 (su1006)]* (15).

FUDR Treatment

slo-1(ky389) and *slo-1(ky399)* mutants are strongly egg laying-defective (Egl) and mostly die of internal larval hatching by D2. *him-4(rh319)* adult animals usually die of explosion from the vulva, a consequence of egg laying through a weakened uterine-vulval structure in this mutant. To circumvent these problems and obtain adult animals at older ages, we treated these mutants with 5-fluoro-2-deoxyuridine (FUDR) to prevent progeny production (16). Animals were placed as L4 on regular bacterial feeding plates with 20 mM FUDR. FUDR at this concentration effectively eliminated all progeny production and did not affect animals' lifespan or neuronal morphology in wild type controls.

Immunofluorescence Microscopy

Immunostaining was performed as described previously (17). Primary antibodies were mouse monoclonal anti-acetylated a-tubulin antibody 6-11B-1 (1: 100, Santa Cruz Biotech) (18) or rabbit polyclonal Rab7 antibody (1: 200, a gift from Dr. Barth Grant, Rutgers University, Piscataway, NJ), and secondary antibodies were 1% Alexa488- and Alexa568-conjugated goat anti-rabbit or goat anti-mouse antibodies (Molecular Probes). Animals were counter-stained with DAPI for better cell recognition. Images were acquired under the Zeiss Axioskop or Zeiss LSM510 confocal microscope.

1. Haithcock E, et al. (2005) Age-related changes of nuclear architecture in Caenorhabditis elegans. *Proc Natl Acad Sci USA* 102:16690–16695.
2. Hsu AL, Murphy CT, Kenyon C (2003) Regulation of aging and age-related disease by DAF-16 and heat-shock factor. *Science* 300:1142–1145.
3. Hajdu-Cronin YM, Chen WJ, Sternberg PW (2004) The L-type cyclin CYL-1 and the heat-shock-factor HSF-1 are required for heat-shock-induced protein expression in Caenorhabditis elegans. *Genetics* 168:1937–1949.
4. Chelur DS, et al. (2002) The mechanosensory protein MEC-6 is a subunit of the C. elegans touch-cell degenerin channel. *Nature* 420:669–673.
5. Clark SG, Chiu C (2003) C. elegans ZAG-1, a Zn-finger-homeodomain protein, regulates axonal development and neuronal differentiation. *Development* 130:3781–3794.
6. Avery L (1993) The genetics of feeding in Caenorhabditis elegans. *Genetics* 133: 897–917.
7. Riddle DL, Swanson MM, Albert PS (1981) Interacting genes in nematode dauer larva formation. *Nature* 290:668–671.
8. Chalfie M, Sulston J (1981) Developmental genetics of the mechanosensory neurons of Caenorhabditis elegans. *Dev Biol* 82:358–370.
9. Vogel BE, Hedgecock EM (2001) Hemicentin, a conserved extracellular member of the immunoglobulin superfamily, organizes epithelial and other cell attachments into oriented line-shaped junctions. *Development* 128:883–894.
10. Henderson ST, Johnson TE (2001) daf-16 integrates developmental and environmental inputs to mediate aging in the nematode Caenorhabditis elegans. *Curr Biol* 11:1975–1980.
11. Wang ZW, Saifee O, Nonet ML, Salkoff L (2001) SLO-1 potassium channels control quantal content of neurotransmitter release at the C. elegans neuromuscular junction. *Neuron* 32:867–881.
12. Troemel ER, Sagasti A, Bargmann CI (1999) Lateral signaling mediated by axon contact and calcium entry regulates asymmetric odorant receptor expression in C. elegans. *Cell* 99:387–398.
13. Sieburth D, et al. (2005) Systematic analysis of genes required for synapse structure and function. *Nature* 436:510–517.
14. Chalfie M, Au M (1989) Genetic control of differentiation of the Caenorhabditis elegans touch receptor neurons. *Science* 243:1027–1033.
15. Gaglia MM, Kenyon C (2009) Stimulation of movement in a quiescent, hibernation-like form of Caenorhabditis elegans by dopamine signaling. *J Neurosci* 29:7302–7314.
16. Hosono R (1978) Sterilization and growth inhibition of Caenorhabditis elegans by 5-fluorodeoxyuridine. *Exp Gerontol* 13:369–374.
17. Finney M, Ruvkun G (1990) The unc-86 gene product couples cell lineage and cell identity in C. elegans. *Cell* 63:895–905.
18. Siddiqui SS, Aamodt E, Rastinejad F, Culotti J (1989) Anti-tubulin monoclonal antibodies that bind to specific neurons in Caenorhabditis elegans. *J Neurosci* 9: 2963–2972.

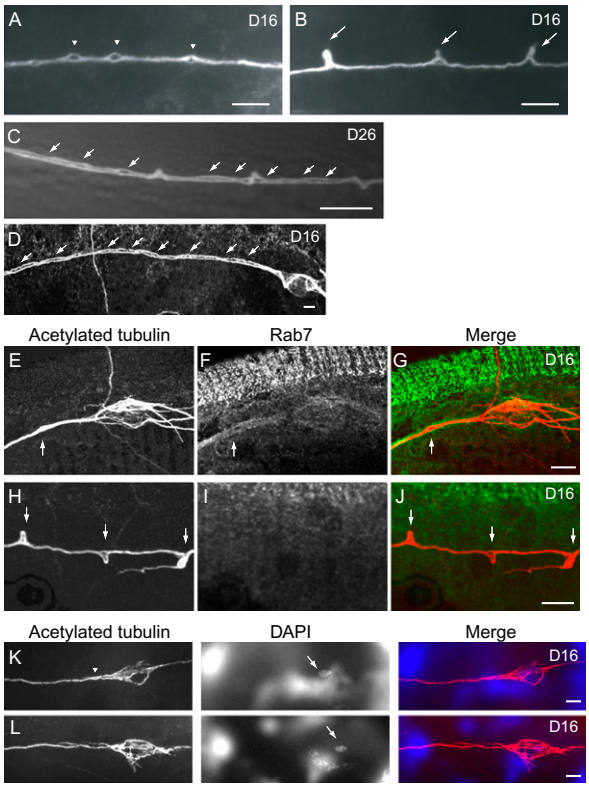

Fig. S1. Age-dependent morphological defects of touch receptor neurons in wild-type animals. Ages (days of adulthood) are indicated. (Scale bar: 5 μm.) (*A* and *B*) 6–11B-1 staining shows bubble-like lesions (*A*, arrowheads) and blebs (*B*, arrows) in the PLM processes. (*C* and *D*) Signs suggesting splitting of touch neuron processes in the PLM (*C*, epifluorescence) and the ALM (*D*, 6–11B-1 staining). Arrows indicate sites of splitting. (*E–J*) Confocal images of double immunostaining for acetylated α-tubulin (*E* and *H*, 6–11B-1) and lysosomes (*F* and *I*, anti-Rab7). Arrows indicate a beading in the ALM process (*E–G*) or blebs in the PLM process (*H–J*). These lesions are not colabeled with anti-Rab7, as shown in the merged images (*G* and *J*). Robust Rab7 immunoreactivity could be seen in the body-wall muscles (*F* and *G*). (*K* and *L*) Double labeling for acetylated α-tubulin (*Left* panels, 6–11B-1) and nuclear DNA (*Center* panels, DAPI) shows that even in aged ALM neurons with marked cytoskeletal defects, the nuclei seem to be intact. The arrowhead in *K* indicates a bubble-like lesion in the ALM process.

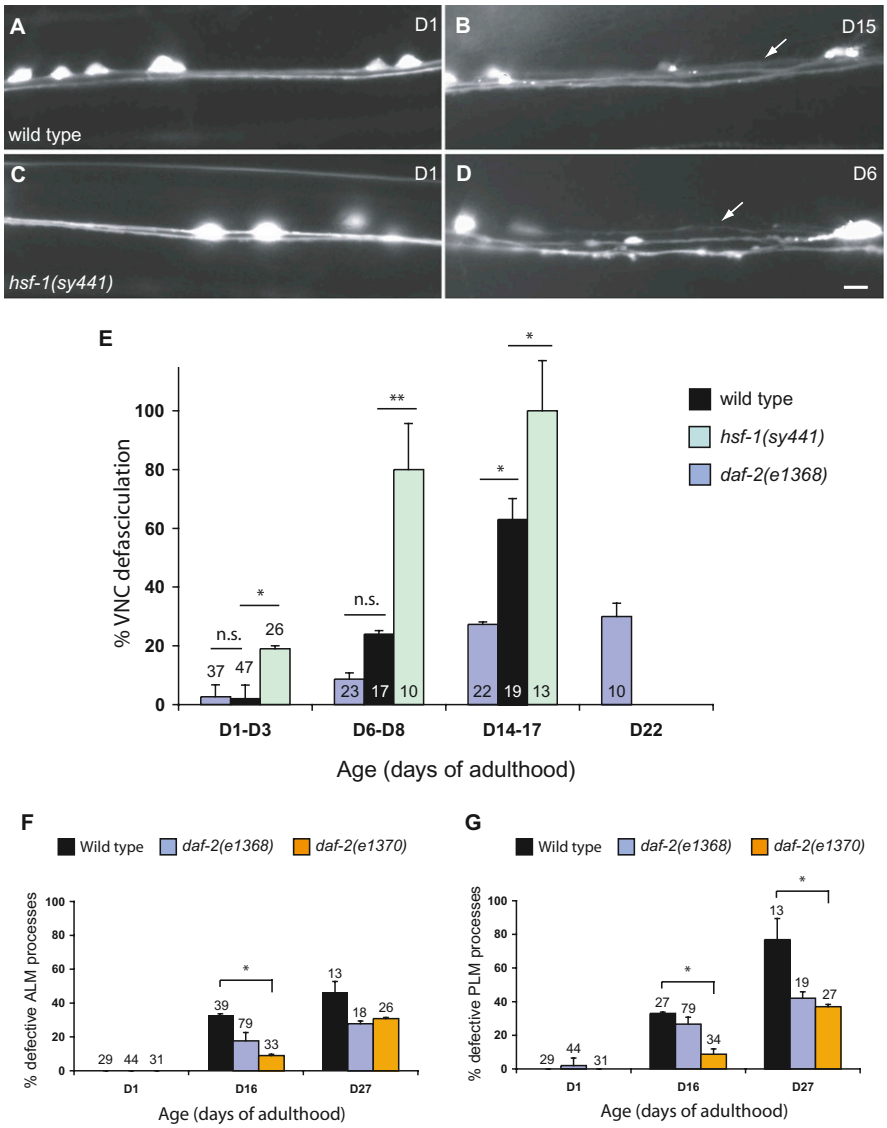

Fig. S2. Age-dependent defects of ventral nerve cord (VNC) axons and touch neurons in wild type and mutants. (Scale bar = 5 μm.) (*A–D*) Epifluorescence images of wild-type (*A* and *B*) and *hsf-1(sy441)* mutants (*C* and *D*), in which VNC cholinergic axons were labeled with the reporter *Punc-17::rfp*. Anterior is to the left, with the right side down and the left side up. Arrows indicate defasciculated axons. (*E*) Quantification of VNC defasciculation in wild-type, *hsf-1 (sy441)*, and *daf-2(e1368)* mutants. (*F* and *G*) Quantification of age-dependent ALM (*F*) and PLM (*G*) defects in wild type, *daf-2(e1368)*, and *daf-2(e1370)* mutants. *daf-2(e1370)* is a stronger allele than *daf-2(e1368)* in terms of life-span extension and constitutive dauer formation. Error bars: SEs of proportions. $*P < 0.05$; $**P < 0.01$; n.s., nonsignificant (Fisher's exact test).

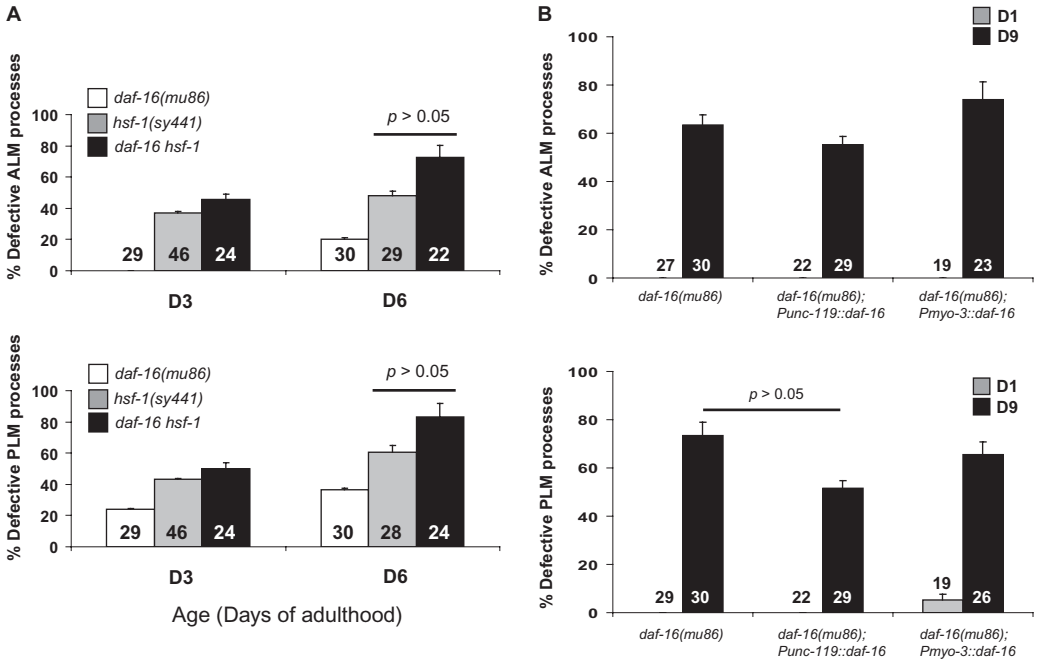

Fig. S3. (*A*) Age-dependent touch neuron defects in the *daf-16(mu86) hsf-1(sy441)* double-mutant animals. Numbers are neurons scored for each genotype at defined ages. *P* is calculated using the two-proportion test. (*B*) DAF-16 functions outside the nervous system to regulate neuronal integrity during normal aging. Bars indicate the percentages of defective neuronal processes for D1 (gray) or D9 (black) animals. Numbers are neurons scored for each genotype at defined time points. *P* is calculated using the two-proportion test. The integrated transgene *muIs131(Punc-119::daf-16)* expresses DAF-16 in the nervous system, and the integrated transgene *muIs126(Pmyo-3::daf-16)* expresses DAF-16 in the body-wall muscles. Both transgenes were kindly provided by Cynthia Kenyon (University of California San Francisco, San Francisco, CA).

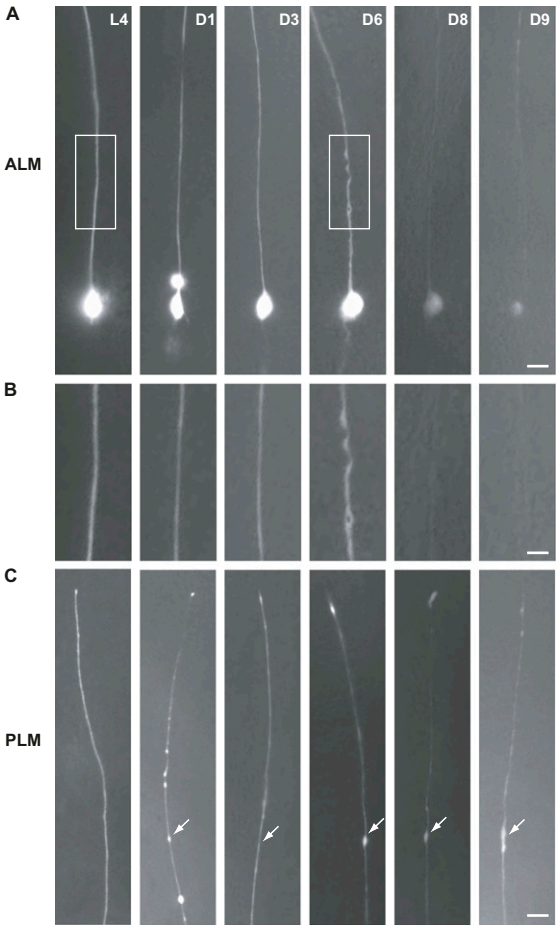

Fig. S4. Longitudinal imaging of progressive ALM and PLM defects in the *hsf-1* mutants. Epifluorescence images of an ALM (*A* and *B*) and a PLM (*C*) touch neuron in the *hsf-1(sy441)* animals at different time points over the animal's life span (lateral view; anterior is up and ventral side to the right). GFP is *zdIs5 (Pmec-4::gfp)*. Age of the animal is indicated as days of adulthood. [Scale bar: 5 μm (*A* and *C*) or 2.5 μm (*B*).] (*A* and *B*) Progressive ALM defects. The ALM process became thinner on D3, compared with that at L4 stage. Irregularity with a bubble-like lesion developed on D6 (*Insets*), and the process gradually disintegrated following D8. The animal died on D10. (*B*) Enlarged images of the *Insets* in the *Upper* panels. (*C*) Progressive PLM defects. Only the most distal part of the PLM process is shown. Similar to what occurred in the ALM process, the PLM process also became progressively thinner. Beading developed following D1, followed by irregularity of the process caliber. Arrows indicate a varicosity that became progressively enlarged after D6.

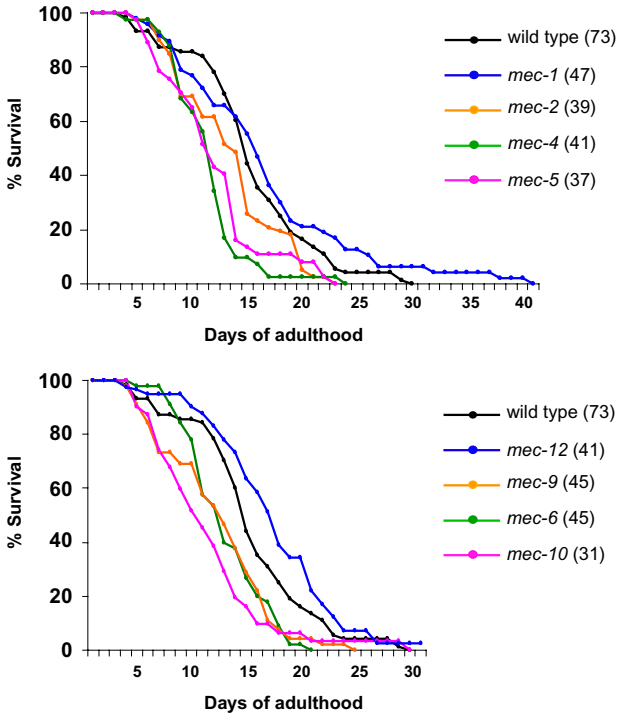

Fig. S5. Life-span assays of the wild-type and various *mec* mutants. Animals were cultured at 20 °C. The number of animals qualified for the life-span assay are in parentheses following each genotype.

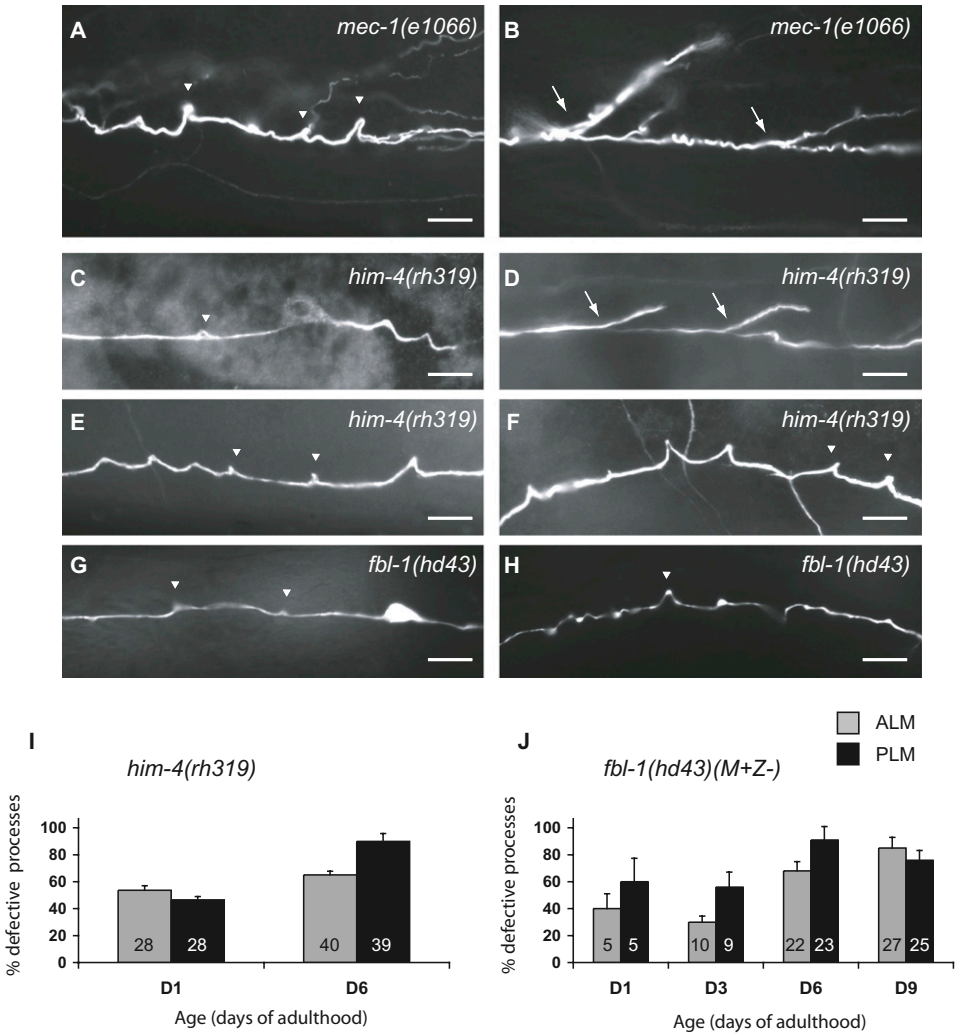

Fig. S6. Blebbing and branching of the ALM processes in the *mec-1*, *him-4*, and *fbl-1* mutants. Immunofluorescence (*A*–*F*) or epifluorescence (*G* and *H*) images of touch neuron processes in the *mec-1(e1066)*, *him-4(rh319),* and *fbl-1(hd43)(M+Z–)* mutants labeled by the 6–11B-1 antibody. Arrows and arrowheads indicate branching and blebbing, respectively. (Scale bar: 10 μm.) (*A* and *B*) ALM in D9 *mec-1(e1066)*. (*C*–*F*) *him-4(rh319)* on D1 (*C* and *E*) and on D5 (*D* and *F*). The phenotypes of ALM (*C* and *D*) and PLM (*E* and *F*) are highly reminiscent of those in *mec-1*. (*G* and *H*) *fbl-1(hd43)(M+Z–)* on D6, with ALM (*G*) and PLM (*H*) developing blebbing and beading. (*I*) Quantification of touch neuron defects in *him-4* mutants. (*J*) Quantification of touch neuron defects in *fbl-1(M+Z–)* mutants. Error bars are SEs of proportions.

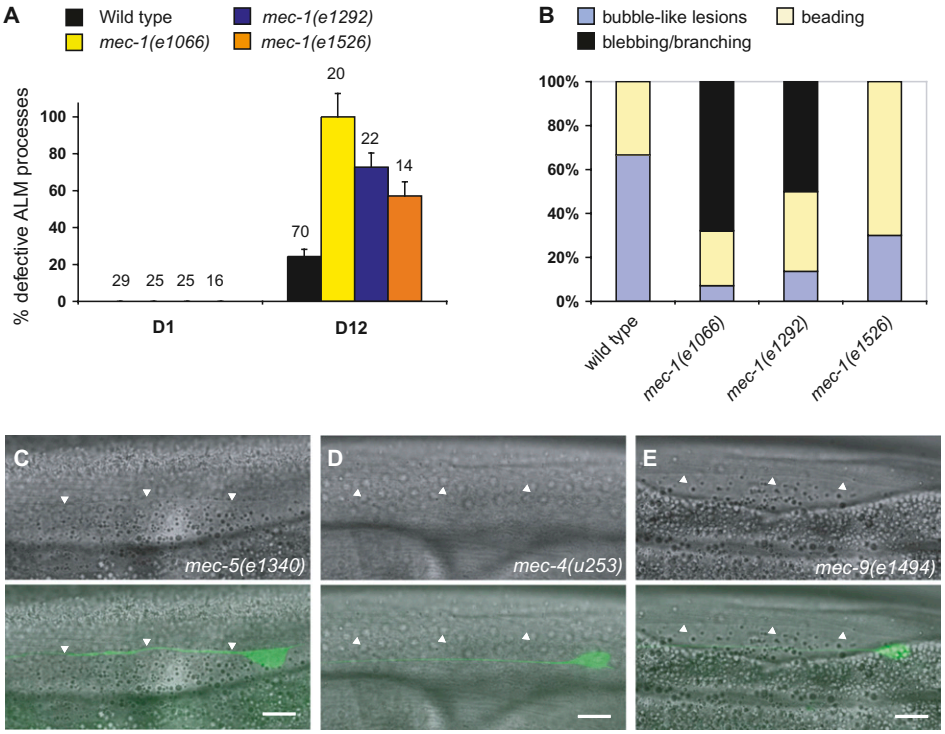

Fig. S7. Touch neuron defects in mutants with defective nerve attachment. (Scale bar: 10 μm.) (*A*) Quantification of defective ALM processes in wild-type and various *mec-1* mutant alleles at D1 and D12. (*B*) Percentages of bubble-like lesions, beading, or blebbing/branching formation in all of the abnormal events found in D12 wild-type and various *mec-1* mutant alleles. (*C–E*) Attachment of the ALM process in *mec-5* (*C*), *mec-4* (*D*), and *mec-9* (*E*) mutants. (*Upper* panels) Differential interference contrast (DIC) images. (*Lower* panels) Overlay of DIC and GFP images of ALM touch neurons. The inferior borders of body-wall muscles are indicated by arrowheads.

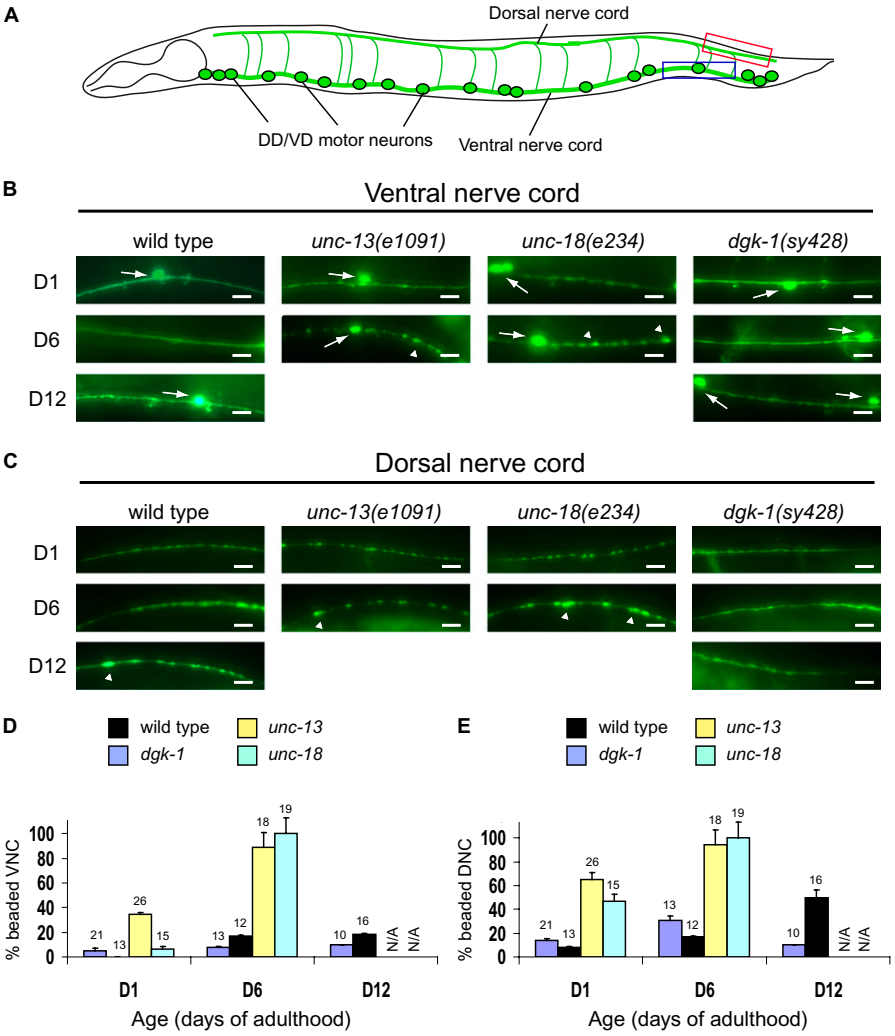

Fig. S8. Altered synaptic transmission influences the integrity of adult GABAergic motor neurons. (*A*) Schematic of the DD and VD GABAergic motor neurons and their axons in the ventral and dorsal nerve cords. The blue and the red boxes mark the regions of morphological assessment in the ventral and dorsal nerve cords, respectively. (*B* and *C*) Epifluorescence images of ventral (*B*) and dorsal nerve cords (*C*) in wild type and mutants with altered synaptic transmission. GFP is from *juIs76(Punc-25::gfp)*. Arrows indicate the cell bodies of the DD or VD neurons, and arrowheads indicate axon beading. (Scale bar: 10 μm.) (*D* and *E*) Quantification of ventral (*D*) and dorsal nerve cord (*E*) beading in wild type and mutants with altered synaptic transmission. Numbers are animals scored. N/A, not assessed.

Table S1. Age-dependent defects of touch receptor neuron processes in wild type and mutants

	% ALM					% PLM				
Age	*N*	Bubble	Blebbing	Beading	Overall	*N*	Bubble	Blebbing	Beading	Overall
					Wild type					
D1	29	0	0	0	0	29	0	0	0	0
D3	51	0	0	0	0	51	0	0	0	0
D6	41	2.4	0	0	2.4	41	0	4.8	4.8	9.8
D9	54	14.8	2	3.7	18.5	54	9.3	13	11.1	26
D12	70	17.1	0	8.6	24.3	100	4	17	16	30
D16	39	33	0	0	33	27	4	26	11	33
D20	19	47.4	0	42.1	63.2	19	15.8	47.4	42.1	73.7
D27	13	38.5	0	23.1	46.2	13	38.5	46.2	61.5	76.9
					hsf-1(sy441)					
D1	20	0	0	15	15	21	0	0	19	19
D3	46	24	2	15	37	46	3	13	24	43.4
D6	29	37.9	3	10	48.3	28	17.8	28.6	25	60.7
D9	23	43.4	0	13	48	23	17.4	30.4	47.8	60.8
D12	21	52.3	5	42.8	76.2	23	17.4	17.4	39.1	56.5
					daf-16(mu86)					
D1	27	0	0	0	0	27	0	0	3.7	3.7
D3	29	0	0	0	0	29	0	17.2	6.9	24.1
D6	30	0	0	20	20	30	0	20	26.7	36.7
D9	30	16.7	3.3	63.3	63.3	30	0	10	66.7	73.3
D12	27	22.2	11.1	30	48	27	0	62.9	33.3	85.2
					daf-2(e1368)					
D1	44	0	0	0	0	44	0	2	0	2
D3	55	0	0	0	0	55	0	0	5	5
D6	51	0	0	0	0	51	2	2	10	13.7
D9	56	8.9	0	0	8.9	56	12.5	3.6	3.6	17.8
D12	51	9.8	0	0	9.8	51	7.8	7.8	3.9	15.7
D16	79	17.7	0	0	17.7	79	20.3	6.3	3.8	26.6
D20	31	29	3	0	32.2	31	22.6	6.5	3.3	32
D27	18	22.2	0	5.5	27.8	19	10.5	36.8	15.8	42.1